

# Product Formalisms for Measures on Spaces with Binary Tree Structures: Representation, Visualization, and Multiscale Noise \*

D. Bassu  
AIG  
devasis.bassu@aig.com

P. W. Jones  
Yale University  
peterwjones@comcast.net

L. Ness  
Rutgers University  
linda.ness@rutgers.edu

D. Shallcross  
Applied Communication Sciences  
dshallcross@appcomsci.com

October 28, 2016

---

\*This work was partially supported by the AFOSR Program FA9550-10-1-0125 titled “Applications to Network Dynamics of Positive Measures and Product Formalisms: Analysis, Synthesis, Visualization and Missing Data Approximation”. The views and opinions expressed in this article do not reflect those of AFOSR, the Air Force, or the US Government. The third author’s work was also partially enabled by DIMACS through support from the National Science Foundation under grant NSF-CCF-1445755.

# Contents

<b>1</b>	<b>Introduction</b>	<b>3</b>
<b>2</b>	<b>Product Formula Representation of Measures on Dyadic Sets</b>	<b>4</b>
2.1	Dyadic sets and product coefficient parameters . . . . .	4
2.1.1	Product coefficients for measures on general trees . . . . .	5
2.2	Dyadic product formula representation lemma . . . . .	5
2.3	Links between product coefficients and standard statistics . . . . .	7
2.4	Exploiting product coefficient parameters for inference and decision . . . . .	7
2.5	Examples of product formula measures . . . . .	8
2.5.1	Borel measures on the unit hypercube . . . . .	8
2.5.2	The product formula representation of a Dirac measure on the unit interval . . . . .	9
2.5.3	Product formula measures determined by feature sets . . . . .	9
2.5.4	Wind example: color displays of product coefficients . . . . .	10
2.5.5	IP data example: source classification using product coefficients as features . . . . .	10
<b>3</b>	<b>Measure Visualization</b>	<b>12</b>
3.1	Background on welding curves and quasi-conformal mapping theory . . . . .	12
3.2	Measure visualization theorem . . . . .	14
3.3	Example: pseudo-welding curves for LIDAR data counting measures . . . . .	15
<b>4</b>	<b>Multiscale Noise Model</b>	<b>17</b>
4.1	Definition of a Dyadic Multiscale Noise Model . . . . .	17
4.2	Multscale noise model theorem . . . . .	17
<b>5</b>	<b>Summary</b>	<b>18</b>
<b>6</b>	<b>References</b>	<b>18</b>

# 1 Introduction

In this paper we focus on measures defined on dyadic sets which are sets with an ordered binary tree of subsets. An example is the partition of the unit interval into dyadic subintervals. The measures are defined on the sigma algebra generated by the subsets in the binary tree. We present three types of theoretical results based on theorems of Fefferman, Pipher and Kenig[16], Beurling and Ahlfors[5], Ahlfors[1], and Kahane[25][36] to obtain a dyadic product formula representation lemma, a visualization theorem, and a multi-scale noise theorem for these measures. The dyadic product formula representation lemma provides an explicit set of product coefficient parameters which are sufficient to distinguish measures on dyadic sets. The visualization theorem shows that measures whose product coefficient satisfy a mild condition can be represented by plane Jordan curves and characterizes the uniqueness of the representing curves. The multiscale noise theorem shows that there is a multiscale noise model for measures on dyadic sets which produces measures in the same family, i.e. measures on dyadic sets with finite non-zero volume, even when the binary tree of dyadic sets is infinite.

Our first contribution is to formulate these three mathematical results in terms of a common statistical parameter, the product coefficient parameter. The three theorems then provide a mathematical basis for a new algorithmizable multi-scale methodology for representation of a broad class of real world data sets as measures, for representation of these measures as Jordan plane curves, enabling visualization of the data, and for representation of multi-scale noise models for the measures as measures in the same family. Representation, visualization, and noise models are fundamental problems in data analysis, They are not typically addressed by a single mathematically based approach. Our second contribution is to algorithmize the methodology and illustrate it in examples and summaries of several applications to real world network and sensor data. Descriptions of the numerical algorithms are available in [4] (Appendix 3). The applications illustrate the utility of the methodology for supervised and unsupervised machine learning.

The dyadic product formula representation was first made explicit for the unit interval in the 1991 Annals of Math paper “The Theory of Weights and the Dirichlet Problem for Elliptic Equations” authored by R. Fefferman, C. Kenig and J. Pipher [16] (Weights are positive functions.) In this paper the authors were trying to prove that certain weights (“harmonic measures”) arising in elliptic PDE lie in the Coifman Fefferman class  $A_\infty$ . (For background on the structure of  $A_p$  weights see [20].) They noted that the  $A_\infty$  condition holds if and only if the measure is doubling and a certain  $L^2$  condition is satisfied for the coefficients. That situation is very far from the case of general measures and in particular the  $L^2$  condition they studied does not hold for multifractal measures which typically arise in for many real data sets including streaming data, images, and videos. Kolaczyk and Nowak also researched multiscale probability models [26]. They give a version of the product formula representation for general measures and not just dyadic trees on Euclidean space. Our focus is the dyadic case and the methodology for representation, visualization and noise models. The multi-scale representation of non-negative measures provided by the product formula is reminiscent of wavelet representation of functions. The key difference is that it applies to measures on dyadic sets and provides a multiplicative representation of non-negative measures parameterized by a normalized set of multi-scale parameters.

Our visualization theorem exploits deep results due to Beurling and Ahlfors [5] and Ahlfors [1] from the theory of quasi-conformal mapping. The results enable construction of a Jordan plane curve (a welding curve) from a measure on the unit circle satisfying mild constraints on its product coefficient parameters and characterize its uniqueness. The product coefficient parameters in the dyadic product formula representation of the measure permit a simple method for constructing a pseudo-welding curve approximating to first order the welding curve determined by the measure. The algorithm for constructing the pseudo-welding curve is given in [4] (Appendix 3). Mumford and Sharon [31] used welding maps to establish a relationship between the 2D shape classes of infinitely smooth Jordan curves and the diffeomorphism classes of their welding maps. Our visualization theorem applies to a much larger class of measure than the class of measures determined by the shape classes of infinitely smooth Jordan curves.

We exploit the multiplicative model of chaos defined by Kahane[25] [36] to define a multi scale noise model for measures. We exploit the analysis in Kahane’s proof to obtain noisy measures with finite, non-zero volume. This noise model is related to Brownian motion. Recent work by Grebenkov, Beliaev and Jones

[18] provides an exposition of Lévy’s formulation of Brownian motion in terms of explicit dyadic multi scale formalisms. They revise Lévy’s construction of Brownian motion to operate with various Gaussian processes. A Brownian path is explicitly constructed as a linear combination of dyadic “geometrical features” at multiple length scales with random weights. Such a representation gives a closed formula mapping of the unit interval onto the functional space of Brownian paths.

## 2 Product Formula Representation of Measures on Dyadic Sets

### 2.1 Dyadic sets and product coefficient parameters

We define a *dyadic set*  $X$  to be a set which has an ordered binary set system consisting of disjoint left and right child subsets for each parent set, whose union is the parent set. The set  $X$  is a parent set and the root of the ancestor tree. A binary set system can be finite or infinite. A binary set system determines a binary tree whose nodes are the sets in the binary set system. Sometimes we will refer to the sets in the binary set system as the dyadic (sub)sets of  $X$ . A *positive measure*  $\mu$  on a sigma algebra generated by a binary set system for the dyadic set  $X$  is determined by an additive non-negative function on sets in the binary set system with the constraint  $\mu(X) > 0$ . In other words, the measure of the left child  $L(S)$  plus the measure of the right child  $R(S)$  is the measure of their parent  $S$ .

$$\mu(L(S)) + \mu(R(S)) = \mu(S)$$

Thus positive measures never take negative values on sets in the sigma algebra generated by the the sets in the binary set system, but even if the measures of all sets in an infinite binary set system are positive there may be sets in the generated sigma algebra whose measure is zero (e.g. the measure of a point in the unit interval is zero even though the measures of all of the dyadic intervals is positive). This is because the sigma algebra contains all sets generated from sets in the binary set system by countable union, countable intersection and complementation. If the total volume of the measure is 1, the measure determines a probability distribution on the sigma algebra of sets generated by the sets in the binary set system. The simplest such measure is the naive measure  $dy$  which assigns  $dy(X) = 1$  and assigns to the left and right children half the measure of their parent .

$$dy(L(S)) = \frac{1}{2}dy(S)$$

$$dy(R(S)) = \frac{1}{2}dy(S)$$

The dyadic product formula representation for a measure  $\mu$  on a dyadic set  $X$  is a product of factors  $1 + a_S h_S$ . There is one factor for each parent set  $S$  (i.e. each non-leaf set) in the binary set system. In the factor  $1 + a_S h_S$ ,  $h_S$  is a Haar-like function defined to have value 1 on  $L(S)$ ,  $-1$  on  $R(S)$ , and 0 on  $X - S$ . In each factor  $a_S$  is the *product coefficient parameter* defined as a solution to the following equations:

$$\mu(L(S)) = \frac{1}{2}(1 + a_S)\mu(S) \tag{1}$$

$$\mu(R(S)) = \frac{1}{2}(1 - a_S)\mu(S) \tag{2}$$

A unique solution to the equations exists if  $\mu(S) \neq 0$ . If  $\mu(S) = 0$  the solution is not unique. To make the product coefficients unique we adopt the convention that whenever one of the “halves” of a binary set has measure zero, the product coefficients for all of the descendant sets of the zero measure “half” have zero product coefficients. This convention implies that if  $\mu(S) = 0$  the solution  $a_S = 0$  is chosen.

The product coefficient  $a_S$  is the amount by which the relative (conditional) measure of the left “half” of  $S$  exceeds the relative (conditional) measure of the right “half” of  $S$ . The use of relative/conditional measure rather than absolute measure means that the product coefficients are self-rescaling. The product coefficients are bounded:

$$-1 \leq a_S \leq 1 \tag{3}$$

Note  $|a_S| = 1$  only if either  $\mu(L(S)) = 0$  or  $\mu(R(S)) = 0$  (but not both).

### 2.1.1 Product coefficients for measures on general trees

If a set  $X$  has an ordered set system with an ordered tree structure in which the root set is  $X$  and the child sets for a parent set are disjoint whose union is the parent set, we will say that the set  $X$  has a tree set system. A positive measure  $\mu$  on the sigma algebra generated by the sets in the tree set system is determined by an additive non-negative function on the sets in the tree set system. We can define a set of  $n$  product coefficients for a parent set  $S$ , which has  $n$  children  $C_i, i = 1 \dots n$ , as the solution to the system of equations

$$\mu(C_i) = \frac{1}{n}(1 + x_i)\mu(S), i = 1 \dots n$$

$$\sum_i^n x_i = 0$$

If the tree is an ordered binary tree, the two product coefficients are additive inverses of each other and the convention we use in the previous section chooses the first one. For the remainder of the paper we will focus on dyadic sets.

## 2.2 Dyadic product formula representation lemma

**Lemma 2.1** (Dyadic Product Formula Representation). *Let  $X$  be a dyadic set with a binary set system whose non-leaf sets are  $\mathcal{B}$ . Let  $\mathcal{B}_n$  denote the non-leaf dyadic sets which are at distance at most  $n$  from the root  $X$  of the dyadic set system.*

1. *If  $\mu$  is a positive measure on  $X$  with product coefficients  $a_S, S \in \mathcal{B}$ , the weak star limit*

$$\mu(X) \prod_{S \in \mathcal{B}} (1 + a_S h_S) dy$$

*of the partial product measures*

$$\mu_n = \prod_{S \in \mathcal{B}_n} (1 + a_S h_S) dy.$$

*exists and*

$$\mu = \mu(X) \prod_{S \in \mathcal{B}} (1 + a_S h_S) dy$$

2. *For any assignment of parameters  $a_S$  from  $(-1, 1)$  and choice of  $\mu(X) > 0$  the weak star limit*

$$\mu(X) \prod_{S \in \mathcal{B}} (1 + a_S h_S) dy$$

*of the partial product measures*

$$\mu_n = \prod_{S \in \mathcal{B}_n} (1 + a_S h_S) dy$$

*exists. The limit measure is positive on all sets  $S$  in the binary set system; its product coefficients are the parameters  $a_S$  and its total mass (and expected value) is  $\mu(X)$ .*

3. *For any assignment of parameters  $a_S$  from  $[-1, 1]$  and choice of  $\mu(X) > 0$  the weak star limit*

$$\mu(X) \prod_{S \in \mathcal{B}} (1 + a_S h_S) dy$$

*of the partial product measures*

$$\mu_n = \prod_{S \in \mathcal{B}_n} (1 + a_S h_S) dy$$

exists. The limit measure is positive; its total mass (and expected value) is  $\mu(X)$ . If the parameters are assigned using the convention that zero value parameters are assigned to the descendant of "halves" of a binary set with zero measure, the parameters are the product coefficients.

*Proof.* The dyadic product formula for non-negative measures using these factors appeared in [16] for  $X = [0, 1]$  and its dyadic intervals of length  $2^{-k}$ ,  $k = 0, 1, \dots$ . We follow their proof to show that it is valid for the more general case of dyadic sets. Let  $\mathcal{B}_n$  denote the non-leaf dyadic sets which are at distance at most  $n$  from the root  $X$  of the dyadic set system. We first prove the second and third parts of the Lemma. For any assignment of parameters  $a_S$  from  $[-1, 1]$  the partial product formula

$$\prod_{S \in \mathcal{B}_n} (1 + a_S h_S) dy.$$

determines a probability measure  $\mu_n$  on the sigma algebra determined by the dyadic set system  $\mathcal{B}_n$  and its child nodes. Because the probability measures  $\mu_n$  all have the same total volume, they converge in the weak- $\star$  sense to a probability measure  $\mu$  on the original dyadic set system. And this probability measure  $\mu$  has the product formula

$$\mu = \prod_{S \in \mathcal{B}} (1 + a_S h_S) dy$$

which is infinite if the original dyadic set system tree has infinite depth. The order in the product is assumed to be lexicographic, by depth in the tree and then left to right in the tree for each depth. Let  $S$  denote a leaf set in  $\mathcal{B}_n$ . Then the product formula for  $\mu_n$  implies that

$$\mu_n(L(S)) = \frac{1}{2}(1 + a_S)\mu_n(S) \quad (4)$$

$$\mu_n(R(S)) = \frac{1}{2}(1 - a_S)\mu_n(S) \quad (5)$$

If  $\mu_n(S) > 0$ , the equations have a unique solution, so  $a_S$  is the product coefficient of  $\mu_n$  for  $S$ . If  $\mu_n(S) = 0$ , there is not a unique solution. We adopt the convention that when the measure of one of the "halves" of  $S$  is zero, all of the product coefficients for its descendant intervals are zero. Hence if  $\mu_n(S) = 0$ , this convention chooses the solution  $a_S = 0$ . For  $m > n$ , let  $\mathcal{B}_m^S$  denote the dyadic set system consisting of  $S$  and its descendants in  $\mathcal{B}$  at distance  $m - n$  from  $S$ . Let  $p_m = \prod_{T \in \mathcal{B}_m^S} (1 + a_T h_T)$  denote the function defined

by the product formula for this dyadic set system. It is a constant function on the children of the leaves of  $\mathcal{B}_m^S$ . And let  $dy_n^S$  denote the naive measure on  $\mathcal{B}_m^S$ . Then  $p_m dy_n^S$  is a probability measure (as above) so

$$\mu_m(S) = \mu_n(S) \int_S p_m dy_n^S = \mu_n(S)$$

By the argument above the weak star limit of the product measures  $p_m dy_n^S$  exists and the volume of  $S$  in the limit measure  $\mu(S) = \mu_n(S)$ . Thus

$$\mu(L(S)) = \frac{1}{2}(1 + a_S)\mu(S) \quad (6)$$

$$\mu(R(S)) = \frac{1}{2}(1 - a_S)\mu(S) \quad (7)$$

This implies that for sets of positive measure, the parameters in the product formula are the product coefficients and for sets of zero measure the parameters in the product formula are the product coefficients if the solution is chosen to be zero. This proves the second and third statements in the Lemma. To prove the first part, note the the partial product formula measures  $\mu_n$  with  $a_S$  defined to be the product coefficients of  $\mu$  define measures on  $\mathcal{B}_n$  which equal the restriction of  $\mu$  to  $\mathcal{B}_n$ . Arguing as above these partial product measures converge to a measure which equals  $\mu$  on the dyadic sets which generate the sigma algebra.  $\square$

### 2.3 Links between product coefficients and standard statistics

All of the standard statistics of a measure (e.g., variance, standard deviation, moments, entropies, information dimensions, as well as the Kullback-Liebler divergence) can be computed via algebraic formulas from the product coefficients for a measure. These standard statistics can also be computed for scale  $n$  approximations to a measure. Approximation algorithms for some of these are provided in [4] (Appendix 3).

For example, the variance of each partial product measure

$$\mu_n = \prod_{S \in \mathcal{B}_n} (1 + a_S h_S) dy$$

on a set  $X$  is a polynomial in the product coefficients whose lowest order term is

$$\text{var}(\mu_n)_{\text{degree } 2} = \sum_{s=0}^n \frac{1}{2^s} \sum_{S \in \mathcal{L}_s} a_S^2$$

where  $\mathcal{L}_s$  is the set of scale  $s$  sets, i.e. sets in the binary set system at distance  $s$  from the root  $X$ . The formula implies the following approximations to the variance:  $a_{00}^2$  for  $n = 0$ ;  $a_{00}^2 + \frac{1}{2}(a_{10}^2 + a_{11}^2)$  for  $n = 1$ ; and  $a_{00}^2 + \frac{1}{2}(a_{10}^2 + a_{11}^2) + \frac{1}{4}(a_{20}^2 + a_{21}^2 + a_{22}^2 + a_{23}^2)$  for  $n = 2$ . Here  $a_{ij}$  is the product coefficient for the  $j$ th set (interval) at scale  $i$ .

The variance of a partial product measure thus is the sum of the variances of the simple single scale dyadic measures  $\prod_{S \in \mathcal{L}_s} (1 + a_S h_S) dy$  because

$$\text{var}\left(\prod_{S \in \mathcal{L}_s} (1 + a_S h_S) dy\right) = \frac{1}{2^s} \sum_{S \in \mathcal{L}_s} a_S^2$$

Also note that these simple single scale measures are the products of the even simpler single scale dyadic measures  $(1 + a_S h_S) dy$ , each of which has expected value 1 and variance  $\frac{1}{2^s} a_S^2$ .

$$\text{var}((1 + a_S h_S) dy) = \frac{1}{2^s} a_S^2$$

where  $s$  is the scale of  $S$ . Thus the product coefficients may be viewed as multi-scale signed standard deviations for simple single scale dyadic measures. The product formula theorem shows that any measure  $\mu$  on a dyadic set  $X$  is uniquely determined by its expected value (the total mass) and the signed single scale standard deviations (i.e., product coefficients). Hence the product formula can be viewed as a generalization of the Gaussian measure which is sufficient to characterize all measures on a dyadic set.

The approximation to the variance above also can be used as a weighted square norm for product coefficient vectors (for finite scale measures). We will refer to this as the *multi-scale variance norm*

$$\|\mu\|^2 = \sum_{n=0,1,\dots} 2^{-n} \sum_{\text{scale}(S)=n} a_S^2 \quad (8)$$

The norm determines a distance between product coefficient vectors and hence a distance between measures (with the same total mass).

### 2.4 Exploiting product coefficient parameters for inference and decision

Product coefficients can be computed from data samples and used to infer unknown measures represented by the data samples. For example, given a set of  $n$  samples of points from a dyadic set  $X$  and a method for pre-processing each sample set into measures for each of the dyadic subsets (e.g. counting measure), a set of product coefficients can be computed for each sample. Let  $\mathcal{P}^i = \{a_S^i : S \in \mathcal{B}\}$ ,  $i = 1, \dots, n$  denote the set of product coefficients for the  $n$  samples from the dyadic set  $X$  with binary set system  $\mathcal{B}$ . Taking the point

of view that these are samples of an unknown measure  $\mu$  the product coefficients  $\mathcal{PC} = \{a_S : S \in \mathcal{B}\}$  for  $\mu$  can be approximately inferred simply by averaging.

$$a_S = \frac{1}{n} \left( \sum_{i=1..n} \{a_S^i\} \right) \quad (9)$$

Define  $\mu(X)$  to be the average of the sample volumes of  $X$ .

This simple rule can be used because the product coefficients are in  $[-1,1]$  so their average is also in this interval and hence determines a measure. The product formula model for the approximation of the measure is:

$$\mu(X) = \prod_{S \in \mathcal{S}} (1 + a_S h_S) dy^{\mathcal{S}} \quad (10)$$

The error in this approximation depends on the dyadic sampling strategy. Different pre-processing methods may result in different measures.

Since the product coefficient parameters uniquely distinguish measures determined by samples (after pre-processing the samples into measures) , they can be used as features for decision rules. This application is illustrated in Section 2.5.5 for IP network data and validated by visualization using a low-dimensional diffusion image of the parameter space. It is also summarized in Section 3.3 for LIDAR data. A different representation method for the data may result in different representations of the data as a measure.

## 2.5 Examples of product formula measures

Examples of dyadic product formula representations of measures may be obtained by defining a dyadic structure on a set  $X$  consisting of a binary set system on a set  $X$  and an additive function on the sets in the binary set system.

### 2.5.1 Borel measures on the unit hypercube

A Borel measure on a topological space  $X$  is a measure defined on the sigma algebra generated by the open sets of  $X$ , i.e., on sets generated by the operations of countably infinite unions, countably infinite intersections and complements of open sets. For  $X = [0, 1]$ , the open sets are open intervals  $(a, b)$ .

For  $X = [0, 1]$  define a binary set system  $\mathcal{D}$  consisting of the half open interval dyadic intervals  $I(n, i) = [i2^{-n}, (i+1)2^{-n})$  for  $i = 0, 1, \dots, 2^n - 2$  and the closed dyadic intervals  $I(n, i) = [i2^{-n}, (i+1)2^{-n}]$  for  $i = 2^n - 1$ . Here  $n$  is any non-negative integer. This infinite collection of dyadic intervals collection forms a binary tree:  $L(I(n, i)) = I(n+1, 2i)$  and  $R(I(n, i)) = I(n+1, 2i+1)$ .  $\mathcal{D}$  generates the same sigma algebra as the open sets (via the operations of countable union, countable intersection and complementation). This is the sigma algebra of Borel sets  $\mathcal{B}$ .

The dyadic measure  $dy$  for this binary set system is defined to be the restriction to  $\mathcal{B}$  of the usual Lebesgue measure  $ds$  on  $[0, 1]$  which measures an interval by its length

$$dx((a, b)) = dx([a, b]) \quad (11)$$

$$= dx((a, b]) \quad (12)$$

$$= dx([a, b]) \quad (13)$$

$$= b - a \quad (14)$$

for  $a < b$ .

A scale  $n$  approximation to a Borel measure is determined by a non-negative step function on the dyadic sets of length  $2^{-n-1}$  and the product formula for this measure can be computed using the bottom-up algorithm described in [4] (Appendix 3).

For higher dimensional unit cubes a binary set system can be obtained by successively halving the sets along dimensions  $n, n-1, \dots, 1$  and then iterating this process infinitely. This binary set system generates the Borel sets on the unit cube. There are many other variants of such dyadic sets systems for higher

dimensional cubes. Again, scale  $n$  approximations to the Borel measure are determined by a non-negative step function on the dyadic sets of scale  $n + 1$ .

The product formula representation theorem for these dyadic systems can also be used to explicitly construct Borel measures.

### 2.5.2 The product formula representation of a Dirac measure on the unit interval

The Dirac measure  $\delta_x$  on  $[0, 1]$  with unit mass at  $x \in [0, 1)$  is not a positive Borel measure because it doesn't assign a positive measure to all intervals. For a dyadic interval  $I = I(n, i)$ ,

$$\sigma_x(I) = 1 \text{ if } x \in I \quad (15)$$

$$\sigma_x(I) = 0 \text{ if } x \in I^c = [0, 1] - I \quad (16)$$

Hence the Dirac measure  $\delta_x$  is a non-negative measure on  $\Sigma(\mathcal{S})$ , the sigma algebra generated by the dyadic intervals. Let  $\mathcal{J}_x$  denote the infinite set of dyadic intervals containing  $x$ , so

$$\mathcal{J}_x = \{I(n, i) = [i2^{-n}, (i+1)2^{-n}], i = \text{floor}(2^n x), n = 0, 1, \dots\} \quad (17)$$

For  $I = I(n, i) \in \mathcal{J}_x$ , define  $a_I = \left(-1^{\text{floor}(2^{n+1}x)}\right)$ , so  $a_I = 1$  if  $x$  is in the left half of  $I$  and  $a_I = -1$  if  $x$  is in the right half of  $I$ . With this definition,  $1 + a_I h_I = 0$  on the half of the interval not containing  $x$ . If  $I$  is a dyadic interval and  $x \notin I$ , then there is an ancestor dyadic interval  $J$  of  $I$  in the tree of dyadic intervals, such that  $x \in J$  and  $I$  is in the subtree rooted at the half of  $J$  which does not contain  $x$ . Hence the definition of product coefficients implies that  $a_I = 0$ . Thus all of the product coefficients for  $\delta_x$  are in  $\{\pm 1, 0\}$  and the product formula is

$$\delta_x = \prod_{n=0}^{\infty} \prod_{i=0}^{2^n-1} 1 + a_{I(n,i)} h_{I(n,i)} dx \quad (18)$$

where  $a_I = -1^{\text{floor}(2^{n+1}x)}$  for  $I = I(n, i) \in \mathcal{J}_x$  and  $a_I = 0$  for  $I \notin \mathcal{J}_x$ .

### 2.5.3 Product formula measures determined by feature sets

For a set  $X$ , let  $\mathcal{F}$  be an ordered collection of proper subsets  $F_i \subset X$ , with the property that

$$F_i \in \mathcal{F} \rightarrow (X - F_i) \notin \mathcal{F}, i = 1, 2, \dots \quad (19)$$

and  $F_0 = X$ .

The sets in  $\mathcal{F}$  may be referred to as "features". The features, together with the set  $X$ , determine a binary set system  $\mathcal{B}$  recursively defined by: The set at level 0 is  $X$ ; for a node set  $S$  at level  $i$ ,  $L(S) = F_{i+1} \cap S$  and  $R(S) = (X - F_{i+1}) \cap S$ . Given a measure  $\mu$  on  $\Sigma(\mathcal{B})$  the expression of  $\mu$  as a product formula measure guaranteed by the theorem shows the proportion of the measure in each intersection of first  $n$  feature sets (and their complements) for  $0 \leq n \leq \text{card}(\mathcal{F})$ . Product coefficients computed for samples of  $X$ , using the binary set system determined by the features, form canonical high-dimensional vectors which can be used to infer an approximation to the product formula for the measure determined by the set of features and can be used in decision and learning algorithms. This assumes a pre-processing step which converts samples of  $X$  into dyadic measures on  $X$ , e.g. counting measure on  $X$ . Even though the full binary tree of dyadic sets may be very large, the set of nodes corresponding to non-empty sets for measures determined by real-world samples can be no larger than a constant times the size of the data set. Note that the measure determines a measure on the nerve simplicial complex determined by the features.

The features above can also be viewed as an ordered set of discrete random variables. The binary set system  $\mathcal{B}$  defined above provides a set of generators for the smallest sigma algebra with respect to which all of the random variables are measurable.

The construction above also implies that non-negative measures on countably generated sigma algebras have dyadic product formula representations. For this case, let  $\mathcal{F}$  be an ordered set of generators for the sigma algebra.

### 2.5.4 Wind example: color displays of product coefficients

Product coefficients for measure representing four days of wind speed data from NREL (the National Renewable Energy Laboratory) for a single year, a single location (in New Jersey) and a single elevation were computed for scales 0 to 5. Figure 1 graphs the time series of wind data for the four days. Figure 2 shows the Whitney tiling visualization of the product coefficients for each of the time series for scales 0 through 5. Scale 0 coefficients are color coded (using the jet convention) in the center and the surrounding annuli color code coefficients for scales 1 through 5. Clockwise beginning at the upper left the day wheels visualize the product coefficients for wind series time series for January 16, December 23, March 1, September 27, respectively. The Jan 16 and Dec 23 wind patterns have relatively little variation, so product coefficients are small. The Mar 1 and Sep 27 wind patterns have a minimum in early afternoon so the scale 0 coefficients are  $> 0$  and the first scale 1 coefficient is  $> 0$  while the second scale 1 coefficient is  $< 0$ . The Whitney tiling visualizations reveal that only the first few product coefficients are required to distinguish the shapes of the four time series.

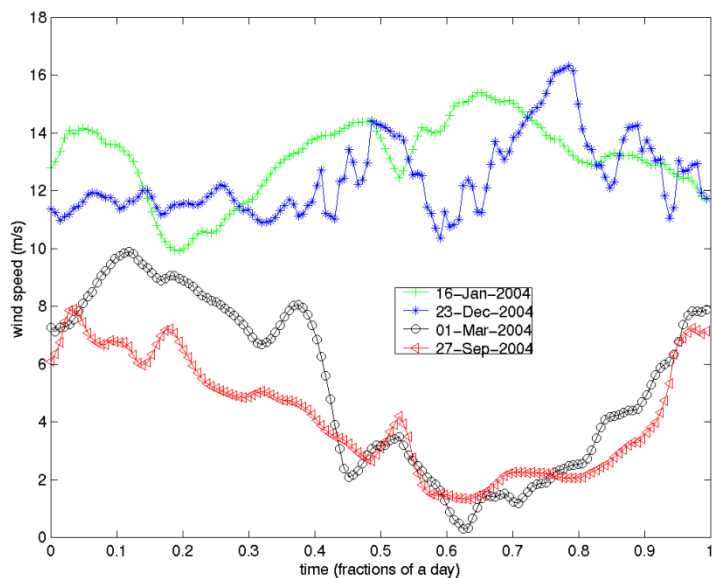


Figure 1: Time Series for 4 Days of Wind Speed Data

### 2.5.5 IP data example: source classification using product coefficients as features

In supervised machine learning the goal is to algorithmically define a classification function using samples of data drawn from a set of unknown probability distributions on the same universe. The classification functions are typically defined on a finite set of features generated from the raw data set using domain knowledge. The measures determined by the feature vectors are typically not characterized. Since the Dyadic Product Representation Lemma applies to all measures on a dyadic set, it is in principle possible to characterize the measures determined by a set of features vectors by computing the product coefficients (to a scale appropriate for the data set) and then use the product coefficients as feature inputs to a classification algorithm. This provides a method for automatically computing a rich set of features sufficient to characterize the measures represented by the samples (to the scale selected). Another challenge is classification using data from multiple sources (i.e. multiple universes). If each source universe has a dyadic structure, data samples from different

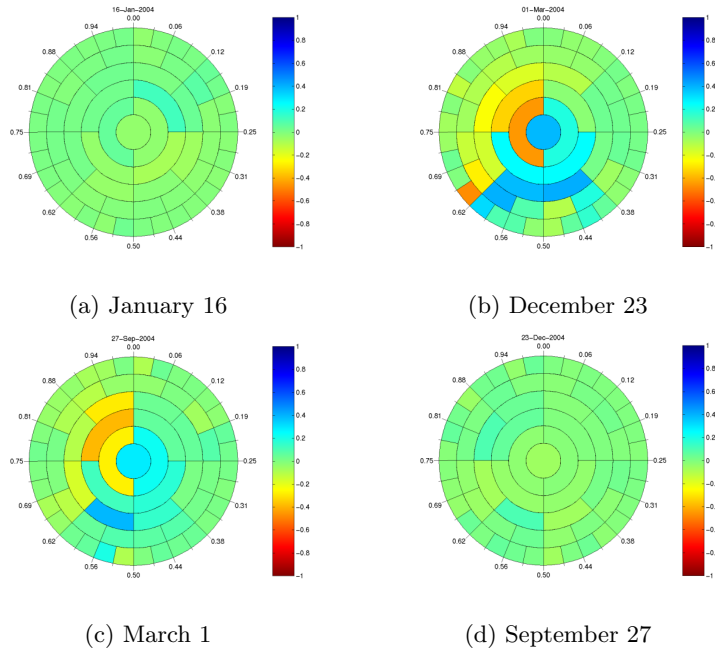


Figure 2: Day Wheel Visualization of the Wind Speed Time Series

universes can each be represented as vectors of product coefficients, whose values all are in the interval  $[0, 1]$ . These product coefficient vectors can be fused by concatenation.

We demonstrated this approach on a data set consisting of IP traffic samples corresponding to port 22 (SSH/SCP service). The question was: would it be possible to construct profiles of the daily traffic which would enable identification of the IP v4 address? In the pre-processing step, twelve raw features signals were computed for each IP address for each day: packets inbound (local), packets outbound (local), bytes inbound (local), bytes outbound (local), degree inbound (local), degree outbound (local), packets inbound (remote), packets outbound (remote), bytes inbound (remote), bytes outbound (remote), degree inbound (remote), degree outbound (remote). Product coefficients were computed for each of the raw signals for scales 0, 1, and 2 so that the finest time interval was 3 hours. They formed an 84-dimensional feature vector per IP per day that represented the daily harmonics for the SSH/SCP service. Each group of 8 product coefficient feature values was normalized so the the product coefficients for each scale were represented equally. For  $L_2$  distance calculations, the assigned weights were: 1 for scale 0 product coefficients,  $\sqrt{1/2}$  for scale 1 product coefficients, and  $1/2$  for scale 2 product coefficients.

The top 6 IPv4 addresses in terms of number of days active were selected. Each of these happened to be from different usage groups identified by the IT staff (but not quantitatively characterized). There were approximately 145 feature vectors for each of the top 6 IP addresses. The Support Vector Machine algorithm was used to compute 6 binary classification functions: one IP address against all of the other IP addresses.<sup>1</sup> The performance for the classification rules was measured in terms of error rate (the probability that the classification is incorrect), sensitivity (the probability that the vector of the targeted class is correctly identified), and specificity (the probability that a vector not belonging to the targeted class is correctly identified). The performance metrics were computed over 10 runs. In each run the data was randomly split into two parts: a training dataset comprised of a randomly selected 75% of the data and the test data set consisting of the remaining 25% of the data. A classification function was computed on the training set and evaluated on the test set. The average results over 10 runs for Support Vector Machine classification using the radial basis kernel are presented in Table 1:

<sup>1</sup>Rauf Izmailov at Applied Communication Sciences did the analysis of the product coefficient data reported in this section.

Averages of Radial Basis SVM Performance Statistics in Percentages			
IPv4 Address ID	Sensitivity	Specificity	Error
ID 1174	93.99	63.68	11.01
ID 2407	97.53	75.48	6.17
ID 1184	95.16	64.21	10.23
ID 2616	97.57	84.69	4.79
ID 1055	99.23	99.07	0.78
ID 2276	97.24	85.14	4.75

Table 1: Radial basis function kernel SVM results

Thus the results implied that for the 6 most active IPv4 addresses it would be practical to approximately infer the IP address IP IDs from the product coefficient representation of the daily activity profile measures. Performance metrics for the linear kernel were significantly worse: e.g. an error rate of 30%+ for IP IDs 1184 and 2276.

The two-dimensional diffusion embedding [13, 14, 30] of the product coefficient vectors in Figure 3 visually illustrates the classification results. The following color map is used: red for IP ID 1055; green for P ID 1174; blue for P ID 1184; yellow for P ID 2276; magenta for IP ID 2407; cyan for IP ID 2616. The figure illustrates the classification results obtained in the previous section by showing which of the classes are easy to separate from others, and which are not so easy to separate (because their measures are more similar). For instance, the best classification result (with its error rate equal to 0.37% for linear SVM and 0.78% for RBF SVM) was obtained for “IP ID 1055 vs all others”. In the diffusion embedding Figures 3, the class 1055 is shown in red, and, indeed, it is fairly easy to see that vectors of this class hardly overlaps with other vectors. The next best classification result (with its error rate equal to 4.57% for linear SVM and 4.79% for RBF SVM) was obtained for “IP ID 2616 vs all others”. In the diffusion embedding shown in Figure 3, class 2616 is shown in cyan, and the vectors of this class, although more overlapping with others than those of class 1055, still are visually distinguishable from other classes. On the opposite end of the classification error rate, as shown in the previous section, one of the worst classification results (with its error rate equal to 32.51% for linear SVM and 10.32% for RBF SVM) was obtained for “IP ID 1184 vs all others”. In the diffusion embedding in Figure 3, the class 1184 is shown in blue, and, indeed, one can see that linear separation of that class from others would be very difficult (which is reflected in poor performance of linear SVM), whereas a curved boundary of RBF SVM decision rule could allow this set of vectors to be classified much better.

Recently, the IP network data was analyzed again using a dyadic tree structured classification algorithm on the set of product coefficients[32].

### 3 Measure Visualization

#### 3.1 Background on welding curves and quasi-conformal mapping theory

As we will show in this section, measures on sigma algebras of binary set systems may be represented (and hence visualized) by Jordan plane curves providing the product coefficient parameters satisfy mild restrictions. Jordan curves are simple closed curves in the plane. We will characterize the uniqueness of these representations. This visualization is guaranteed by several deep mathematical theorems in quasi-conformal mapping theory due to Beurling and Ahlfors [5] and Ahlfors [1].

Let  $\mathcal{D}$  denote the binary set system on  $[0, 1]$  consisting of the half open interval dyadic intervals  $I(n, i) = [i2^{-n}, (i+1)2^{-n})$  for  $i = 0, 1, \dots, 2^n - 2$  and the closed dyadic intervals  $I(n, i) = [i2^{-n}, (i+1)2^{-n}]$  for  $i = 2^n - 1$ .  $\mathcal{D}$  can be viewed as a dyadic set system for the unit circle  $S^1$  (with zero mapped to 1).

A measure  $\mu$  on  $\Sigma(x, \mathcal{S})$  the sigma algebra of a binary set system on  $X$ , uniquely determines a measure  $\mu_{S^1}$  on  $\Sigma(S^1, \tilde{\mathcal{D}})$  (and vice versa). (The measures have the same product coefficients.) We propose to

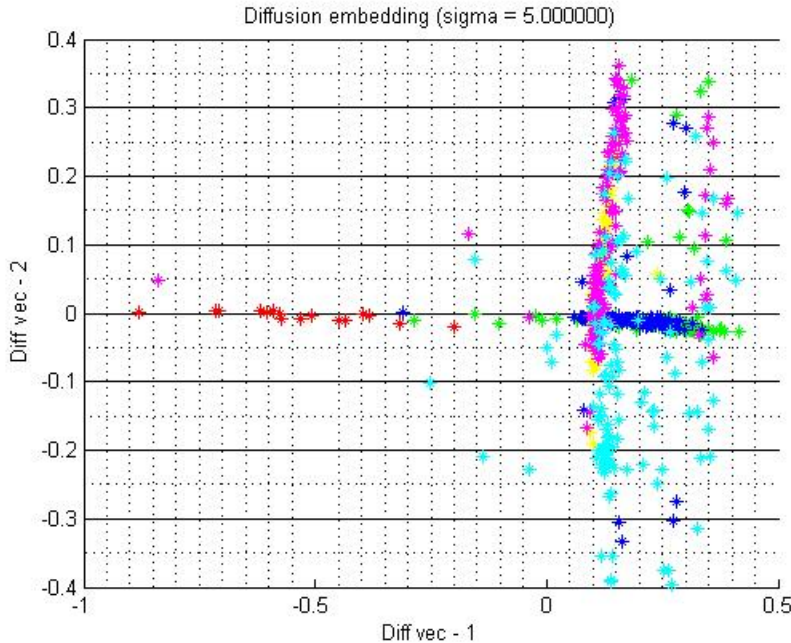


Figure 3: Diffusion embedding (sigma=5).

visualize  $\mu$  by visualizing the measure  $\mu_{S^1}$ . (The previous wind examples shows that measures on sigma algebras generated by binary set systems can alternatively be visualized using Whitney tilings.)

The connection between Jordan curves in the plane and measures is made via the welding map. The welding map for a Jordan curve  $\Gamma$  in the plane is constructed as follows: let  $F_+$  be a choice of conformal map from the unit disk to interior of  $\Gamma$ , and let  $F_-$  be a choice of conformal map from the outside of the unit disc  $\{|Z| > 1\}$  to the domain exterior to  $\Gamma$ . Define  $\Phi = F_-^{-1} \circ F_+$ . Then  $\Phi : S^1 \rightarrow S^1$  is a homeomorphism of the unit circle to itself, and  $\Phi$  is called the **welding map** for  $\Gamma$ . The Jordan curve  $\Gamma$  is a welding curve for  $\Phi$ . Because  $\Phi$  is a homeomorphism its derivative  $\Phi'$  is a positive measure  $\mu$  on the unit circle  $S^1$ , which has positive measure on all intervals of positive length. In fact,  $\Phi'$  is a finite measure if and only if  $\Phi$  has bounded variation. The von Koch snowflake curve is an example of a map of the unit circle whose derivative is not only a singular Lebesgue measure, but in fact has support on a set of Hausdorff dimension less than 1. Okiwa showed the existence of examples of homeomorphisms of the unit circle which are not welding maps [33]. Okiwa proved that if the derivative of a homeomorphism of the unit circle scales like two different powers of  $\theta$  on adjacent intervals of the unit circle it is not a welding map.

The measure determined by the derivative of the welding map  $\Phi$  encodes the geometry of the welding curve  $\Gamma$ . For example, if close to some point  $z_0$  on  $\Gamma$ , the curve looks like two intervals having an interior angle of  $\theta$  at  $w_0$ , then there is a point  $z_0$  on the circle such that

$$\Phi' \sim |z - z_0|^{\frac{2\theta - 2\pi}{2\pi - \theta}} \text{ near } z_0 \quad (20)$$

The converse also holds. This type of power singularity for  $\Phi'$  is also reflected in its coefficients  $a_I$ . See [33] for an early paper with basic properties of welding. Recent works of Astala, Jones, Kupiainen and Saksman [2] provides new, probabilistic classes of welding maps that arise in Conformal Field Theory.

We exploit important facts from quasi-conformal mapping theory to construct a Jordan curve from a positive measure on the unit circle. If a measure  $\mu$  on  $S^1$  satisfies the quasi-symmetric condition, i.e. for all intervals  $I \subset S^1$

$$\frac{1}{C} \leq \frac{\mu(I_L)}{\mu(I_R)} \leq C \quad (21)$$

where  $C > 0$  is independent of  $I$ , where  $I_L$  and  $I_R$  denote the left and right halves of the interval  $I$ , then it is the derivative of a homeomorphism  $\Phi : S^1 \rightarrow S^1$  and the Beurling-Ahlfors extension theorem [5] extends  $\Phi$  to be a quasi-conformal mapping  $F : D \rightarrow D$  from the unit disc to itself which solves the Beltrami equation

$$\bar{\partial}F = \mu\partial F$$

Here  $\mu$  is defined to be identically zero,  $\mu \equiv 0$  off  $D$ , and  $\|\mu\|_\infty \leq 1 - \epsilon(C)$ . It can be shown that  $\Gamma = F(S^1)$  is the welding curve associated to  $\Phi$ . Furthermore, the welding map  $\Phi$  is unique in that any other welding map  $\hat{\Phi}$  whose derivative is  $\mu$  is the welding map for a Jordan curve  $M(\Gamma)$  where  $M : \mathbb{C} \rightarrow \mathbb{C}$  is a Möbius transformation  $z \rightarrow \frac{az+b}{cz+d}$ ,  $ad - bc \neq 0$ . These facts are proved by Lars Ahlfors in the original version of his book ‘‘Lectures on Quasi-Conformal Mappings’’ [1].

Note for finite measures the quasi-symmetric condition on a measure is equivalent to the condition that the absolute values of the product coefficients are strictly bounded away from 1. For measures on sigma algebras determined by an infinite binary system, the quasi-symmetric condition implies the condition that the absolute values of the product coefficients are strictly bounded away from 1. In this case if the absolute values of the product coefficients for both  $\mu_{S^1}$  and  $\mu_{S^1} \circ (\text{rotation by } \frac{2\pi}{3})$  are strictly bounded away from  $\pm 1$  the measure is quasi-symmetric.

## 3.2 Measure visualization theorem

**Theorem 3.1** (Measure Visualization). *For a measure  $\mu$  on  $\Sigma(X, \mathcal{S})$ , the sigma algebra of a binary set system on  $X$ , let  $\mu_{S^1}$  denote the measure on  $\Sigma(S^1, \tilde{\mathcal{D}})$  with the same product coefficients.*

1. *If  $\mu_{S^1}$  is a positive measure represented by a finite product formula and none of its product coefficients are  $\pm 1$ , then  $\mu_{S^1}$  is the derivative of a welding map  $\Phi : S^1 \rightarrow S^1$  determined by a Jordan curve  $\Gamma$ , denoted  $\Gamma_{\mu_{S^1}}$ , unique up to Möbius transformations.*
2. *If  $\mu_{S^1}$  is represented by an infinite product formula, and if the product coefficients for both  $\mu_{S^1}$  and  $\mu_{S^1} \circ (\text{rotation by } \frac{2\pi}{3})$  are strictly bounded away from  $\pm 1$ , (i.e., if there exists  $\epsilon > 0$  such that all product coefficients satisfy  $|a_I| \leq 1 - \epsilon$ ), then  $\mu_{S^1}$  is the derivative of a welding map  $\Phi : S^1 \rightarrow S^1$  determined by a Jordan curve  $\Gamma$ , denoted  $\Gamma_{\mu_{S^1}}$ , unique up to Möbius transformations.*

*Proof notes.* This is a non-trivial theorem usually proved by using  $L^p$  estimates on the Beurling transform which transforms a function  $f : \mathbb{C} \rightarrow \mathbb{C}$  by convolving it with the kernel  $\frac{1}{\pi z^2}$ . This transformation is a bounded operator on the function space  $L^p$  for  $1 < p < \infty$ . For  $L^2$  the norm of this operator is 1. The proof is in the original portion of Ahlfors’ book ‘‘Lectures on Quasi-Conformal Mappings’’ [1].  $\square$

For some measures represented by an infinite product formula which does not satisfy the condition 2 of the Measure Visualization theorem, there exist multiple non-equivalent welding maps [35]. In fact, if the Jordan curve in the plane has positive 2D Lebesgue measure (e.g., a Jordan curve which threads through a Cantor set with positive 2 dimensional Lebesgue measure) then there exist an uncountable number of non-equivalent welding maps. This is discussed in [22]. A deep theorem is: given any closed set of  $\mathbb{R}^2$  of positive measure (e.g., the two sphere  $S^2$ ) there exists a quasi-conformal map  $f : \mathbb{R}^2 \rightarrow \mathbb{R}^2$  that is not a Möbius transformation but is holomorphic off a closed set and one-to-one on the closed set. [1]. The closed set can be used to obtain non-unique welding maps.

The visualization theorem applies to positive measures whose product coefficients are strictly bounded away from 1 in absolute value. To visualize finite real-world measures some of whose product coefficients have absolute value 1, one can deform the product coefficients slightly to obtain a positive measure. The visualization of such a deformation should still reveal the binary sets with measure 0, i.e. the disconnected geometry of the support of the measure.

The discussion preceding the theorem outlines a complex analytic method for computing a welding curve. However, a first order approximation to a welding curve visualizing a measure can be computed quite simply using only the product coefficients for the measure  $\mu$ . We call this approximate visualization curve the *pseudo-welding curve*. An algorithm for computing it is given in [4] (Appendix 3).

An exposition of approaches for constructing welding curves is also given in Mumford and Sharon [31]. Mumford and Sharon[31] were studying 2D shape classes, which they defined to be equivalence classes of (infinitely) smooth Jordan curves, where curves were equivalent if they differed by translation and scaling. They proved that these shape classes are the same as the diffeomorphism classes of the welding maps for the smooth Jordan curves modulo the Möbius transformations and then went on to study the Weil-Peterson metric on the diffeomorphism classes. They give a clear exposition of the existence theory for welding maps and summarize computational methods for welding curves. The class of measures determined by the shape classes is much, much smaller than the class of measures identified in the Visualization Theorem. Most real world measures (including finite approximations to them) do not determine infinitely smooth Jordan curves. Mumford and Sharon’s view point is that all shapes cannot be characterized by a fixed finite number of ”features”. However, if an  $\epsilon > 0$  is chosen, a representative infinitely smooth shape curve can be well approximated by a curve determined by a finite number of product coefficients, where the number of product coefficients depends on both the geometric properties of the curve and the smoothness.

### 3.3 Example: pseudo-welding curves for LIDAR data counting measures

We experimented with applying the product formula representation to a counting measure derived from a set of LIDAR sample data [10]. This data consists of ten sets of discrete points in 3-dimensional space, representing the surfaces visible to the scanning laser rangefinder in ten nearby scenes. Each point has been labelled as either “vegetation” or “ground”. For the most part the ground was wavy, but approximately horizontal, while the vegetation consisted of shrubs, with more vertical extent. Previous work [6] had examined this same data using a multi-scale SVD approach to build a support vector machine (SVM) based classification rule that could, with high accuracy, reproduce the vegetation/ground labelling. We experimented with using product coefficient parameters as features instead of multi-scale SVD parameters. The experiment showed that decision rules for distinguishing two measures (here “vegetation” and “ground”) could be approximately inferred from histograms of the product coefficients. While the metrics were not as good as for multi-scale SVD, the method did provide a transparent rationale for the decision rule.

For our analysis, we translated and scaled the data sets to fit them into the unit cube  $[0, 1]^3$ , and to send their median  $x$ ,  $y$ , and  $z$  coordinates to the same location  $(m_x, m_y, m_z)$  in the cube. Each data set had its own translation vector, but a common set of three scaling factors was chosen. The target median point and the scaling factors were chosen to make the scaling factors as large as possible. We then applied the product form decomposition, subdividing the cube sequentially by dimension 1, 2, 3, 1, 2, 3, etc. to the measure given by point masses of equal weight at each of the data points. While subdividing each dimension 10 times gives 230 coefficients, we only needed to calculate those coefficients that correspond to subdividing a cell containing at least one data point. A full description of the analysis of the LIDAR data is given in Appendix 2 of [4].

We constructed pseudo-welding curves, each a piecewise linear curve between the points (0,0) and (0,1), via a snow-flake like curve construction. The knots of the curve at the  $i^{th}$  scale are obtained by raising or lowering the midpoint of the linear segments of the curve by the value of the corresponding product coefficient weighted by a factor of  $2^{-s}$ . The full algorithm is described in Appendix 3 of [4]. The corners, or knots, of the piecewise linear curves correspond to particular coefficients, and so to the corresponding subsets of the unit cube on which these coefficients represent divisions. We have colored these knots according to the classifications of the LIDAR points contained in the subsets. Red knots correspond to subsets containing only ground points, green knots correspond to subsets containing only vegetation points, blue knots correspond to subsets containing both ground and vegetation points, and black knots correspond to subsets containing no LIDAR points. (Subsets containing no LIDAR points produce coefficients with value zero.) We can see that the pseudo-welding curves for the different samples have similar shapes.

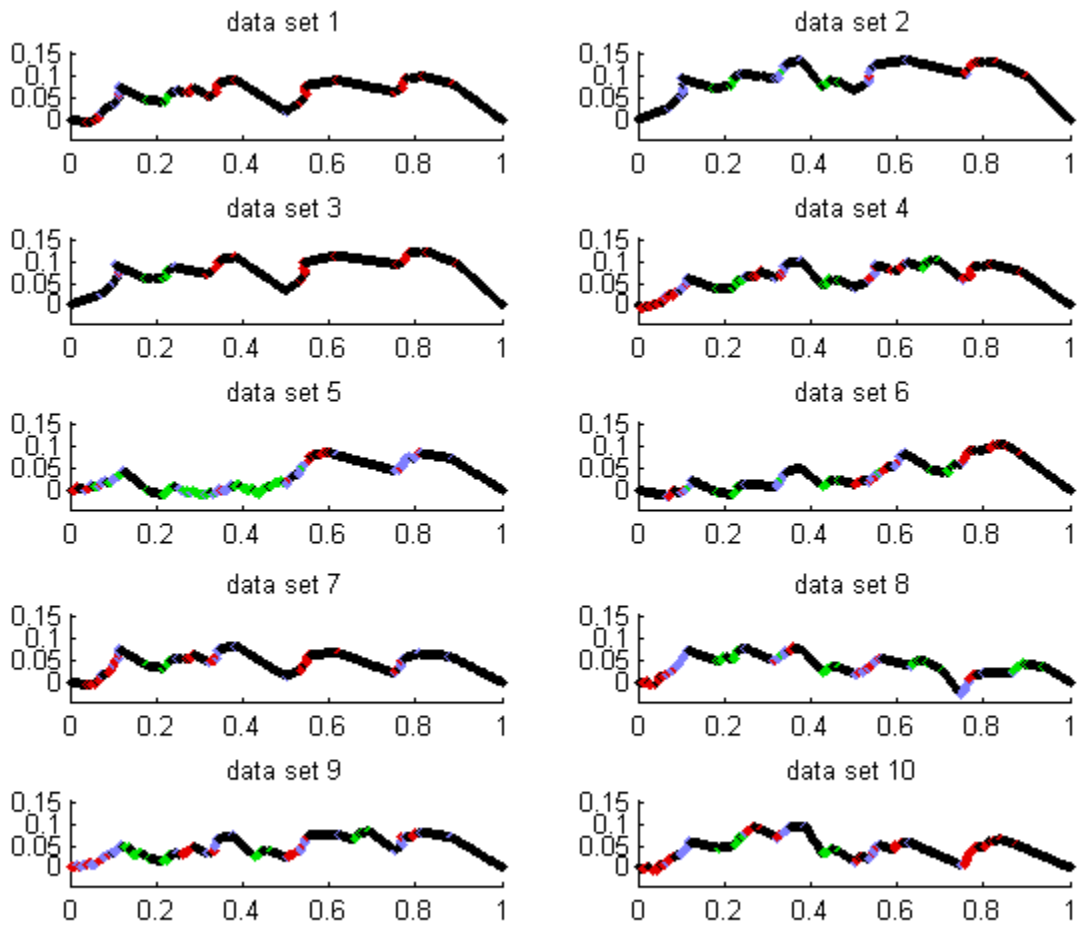


Figure 4: Pseudo-welding curves for the LIDAR data

## 4 Multiscale Noise Model

### 4.1 Definition of a Dyadic Multiscale Noise Model

For the general family of dyadic product formula measures on dyadic sets, very general noise models can be defined which determine other measures in the same family (for each fixed set of noise parameters). The product coefficients any instance of noisy measure could be computed and compared with the original parameters. The mathematical subtlety is formulating such a noise model which has finite and non-zero volume even if the the binary set system is infinite.

Assume we are given a binary set system on a set  $X$ . Let  $\mathcal{B}$  denote the non-leaf node sets and let  $\mathcal{B}_n$  denote the non-leaf node sets at distance at most  $n$  from the root  $X$ . For each scale  $n$  first define a *dyadic multiscale noise function*

$$\mathcal{N}_n(y) = \exp\left(\sum_{S \in \mathcal{B}_n} b_S^n h_S - (\sigma_S^2/2)\chi_S\right)(y)$$

In the definition  $\chi_S$  is the characteristic function for the set  $S$ ,  $\{\sigma_S : S \in \mathcal{B}\}$  is the set of noise parameters for the model and  $\{b_S^n\}$  is the set of noise coefficients for the model. The noise coefficients are independent Gaussian random variables with variance  $\sigma_S^2$ . They are defined by the formula

$$b_S^n = \sigma_S Z_S$$

using a set  $\{Z_S : S \in \mathcal{B}\}$  of independent Gaussian random variables with mean zero and variance 1. If all sets  $S$  with the same scale  $n$  have the same noise parameter  $\sigma_S = \sigma_n$ , the noise model is *scale dependent*.

For each scale  $n$  the noise model function determines a measure  $\mathcal{N}_n(y)dy$  whose expected value (total mass) is obtained by integration over  $X$  (i.e. summation over the level  $n$  sets  $\mathcal{L}_n$  since the noise function for the level is constant on each level  $n$ ). The *dyadic noise model measure*  $\mu_{\mathcal{N}_n}$  for each scale  $n$  is defined to be the probability measure obtained by dividing by the expected value, if the expected value is non-zero and finite.

$$\mu_{\mathcal{N}_n} = \frac{1}{E_n} \mathcal{N}_n(y)dy$$

where

$$E_n = \int_X \mathcal{N}_n(y)dy.$$

The *dyadic multiscale noise model measure*  $\mu_{\mathcal{N}}$  determined by the set of noise parameters  $\{\sigma_S : S \in \mathcal{B}\}$  is then defined to be the weak star limit of the measures  $\mu_{\mathcal{N}_n}$ , if the limit exists. Furthermore if the limit exists, the dyadic product formula representation lemma implies that  $\mu_{\mathcal{N}} = \mathcal{N}dy$ . This  $\mathcal{N}$  is the *dyadic multiscale noise function*. This dyadic noise model function can be used to define a noise model measure  $\mu_{\mathcal{N}}$  for a positive measure  $\mu$  which satisfies mild constraints on their product coefficients. This is made precise in the following Theorem.

### 4.2 Multiscale noise model theorem

**Theorem 4.1** (Multiscale Noise Model ). *Let  $X$  denote a set with a binary set system with non-leaf sets  $\mathcal{B}$  and level  $n$  set  $\mathcal{B}_n$ . Let  $\{\sigma_S : S \in \mathcal{B}\}$  denote a set of noise parameters for  $\mathcal{B}$ .*

1. *If  $\sup\{\sigma^2\} < 2\log(2)$  then almost surely the weak star limit of the measures  $\mu_{\mathcal{N}_n}$  exists and determines a non-zero finite measure  $\mu_{\mathcal{N}} = \mathcal{N}dy$  on  $X$ .*
2. *If  $\mu$  is a positive measure on the the sigma algebra generated by  $\mathcal{B}$  on  $X$  with product formula*

$$\mu = \mu(X) \prod_{S \in \mathcal{B}} (1 + a_S h_S)dy$$

and if  $|(a_S)| \leq 1 - \epsilon$  and  $\sigma^2 < \epsilon/2$ , almost surely the weak star limit of

$$\mu(X) \frac{1}{E_n} \mathcal{N}_n \prod_{S \in \mathcal{B}_n} (1 + a_S h_S) dy$$

exists and determines a finite positive measure  $\mu_{\mathcal{N}}$  on  $X$ .

*Proof.* Part 1 is the dyadic version of a theorem of Kahane [25, 36]. Peter Jones has observed that Kahane’s proof also implies part 2 of the theorem.  $\square$

Following the estimates of Kahane, it can be shown that the expected values of the product coefficients for  $\mu_{\mathcal{N}}$  are approximately the product coefficients of the original measure. The variance of the product coefficients for  $\mu_{\mathcal{N}}$  is bounded by the noise parameters. Formal explicit bounds would permit precision and specificity estimates for decision theorems based on the product coefficients for samples from a noise model for a measure. An algorithm for computing maximum likelihood estimates for several scenarios is given in Appendix C.

The dyadic Gaussian multiscale noise model is a dyadic version of the Gaussian noise model which is related to the Gaussian Free Field. The Gaussian Free Field is an everywhere divergent random sum which has "the same energy at every scale". In all dimensions it can be defined by Fourier Series. Kahane’s surprising result [25, 36], which we exploited in the theorem above, states that if the "variance at each scale" is less than 2, one can subtract infinity, exponentiate it, and get non-zero, finite measures - which we refer to as Gaussian multiscale noise. Brownian motion on the circle  $S^1$  is the restriction of the two dimensional Gaussian Free Field. Recent expository work by Grebenkov, Beliaev and Jones [18] provides an exposition of Lévy’s formulation of Brownian motion in terms of explicit dyadic multiscale formalisms. They revise Lévy’s construction of Brownian motion to operate with various Gaussian processes. A Brownian path is explicitly constructed as a linear combination of dyadic "geometrical features" at multiple length scales with random weights. Such a representation gives a closed formula mapping of the unit interval onto the functional space of Brownian paths.

## 5 Summary

In this paper we focused on positive measures defined on dyadic sets which are sets with an ordered binary tree of subsets. We re-formulated three mathematical results, proved by Fefferman, Pipher and Kenig, Beurling and Ahlfors, and Ahlfors and Kahane, in terms of a single type of statistical parameter, the product coefficient parameter. The mathematical results are valid even if the binary trees are infinite. The re-formulated results provide a mathematical basis for a new algorithmizable multi-scale methodology for representation of a broad class of real world data sets as measures, for representation of these measures as Jordan plane curves, enabling two-dimensional multi-scale visualization of the data, and for representation of multi-scale noise models for the measures as measures in the same family. The approach provides a single mathematically based methodology for data representation, data visualization, and noise models. We algorithmized the methodology. Descriptions of the numerical algorithms are available in [4] (Appendix 3). In this paper we also illustrated the computational methodology in examples and summaries of several applications to real world network and sensor data. The examples illustrate the broad applicability of the approach and provide links to standard statistics. The applications illustrate the utility of the methodology for supervised and unsupervised machine learning.

## 6 References

- [1] Ahlfors, L., *Lectures on Quasi-Conformal Mappings*, van Nostrand Mathematical Studies, vol. 10, 1966.
- [2] Astala, K. & Kupiainen, A. & Saksman, E. & Jones, P., *Random Conformal Weldings*, Acta Mathematica, v. 207(2), pp. 203-254, Dec 2011.

- [3] Barral, J., & Mandelbrot, B., *Multifractal products of cylindrical pulses*, Probability Theory and Related Fields, vol. 124, pp. 409-430, 2002.
- [4] <https://arxiv.org/abs/1601.02946v2>
- [5] Beurling, A. & Ahlfors, L., *The boundary correspondence under quasi-conformal mappings*, Acta Math. 96 (1956), 125-142.
- [6] Bassu, D., & Izmailov, R., & McIntosh, A., & Ness, L., & Shallcross, D., *Centralized Multi-Scale Singular Value Decomposition for Feature Construction in LIDAR Image Classification Problems*, 2013 IEEE Applied Imagery Pattern Recognition Workshop, pp. 1-6, 2012.
- [7] Bishop, C., & Jones, P. W., *Hausdorff dimension and Kleinian groups*, Acta Mathematica Publisher Springer Netherlands ISSN0001-5962 (Print) 1871-2509 (Online) vol. 179, no. 1 / September, 1997, pp. 1-39.
- [8] Bishop, C., & Jones, P. W., *Wiggly sets and Limit sets*, Arkiv fr Matematik, Springer Netherlands ISSN0004-2080 (Print) 1871-2487 (Online) vol. 35, no. 2 / October, 1997, pp. 201-224.
- [9] Bowen, R., *Hausdorff dimension of quasi-circles*, Publications Mathematiques de L'IHS Publisher Springer Berlin / Heidelberg ISSN0073-8301 (Print) 1618-1913 (Online) vol. 50, no. 1 / December, 1979, pp. 11 25.
- [10] Brodu, N., & Lague, D., *3D terrestrial LiDAR data classification of complex natural scenes using a multi-scale dimensionality criterion: applications in geomorphology*, ISPRS Journal of Photogrammetry and Remote Sensing, vol. 16, pp. 121-134, 2012.
- [11] Canary, R. & Minsky, Y. & Taylor, E., *Spectral theory, Hausdorff dimension, and the topology of hyperbolic three manifolds*, Journal of Geometric Analysis, vol. 9, pp. 1740, 1999.
- [12] Chang, A., & Wilson, M., & Wolff, T., *Some weighted norm inequalities concerning Schrodinger operators*, Commentarii Mathematici Helvetici, Publisher Birkha user Basel ISSN0010-2571 (Print) 1420-8946 (Online) Issue vol. 60, no. 1/December, 1985, pp. 217-246.
- [13] Coifman, R. & Lafon, S., *Diffusion maps*, Appl. Comp. Harm. Anal 21 (2006), 5-30.
- [14] Coifman, R. R. & Lafon, S. & Lee, A. B. & Maggioni, M. & Nadler, B. & Warner, F. & Zucker, S. W., *Geometric diffusions as a tool for harmonic analysis and structure definition of data: Diffusion maps*, PNAS, vol. 102 no. 21, pp.74267431, 2005.
- [15] Donoho, D. & Johnstone, I. M., *Minimax estimation via wavelet shrinkage*, Annals of Statistics, vol. 26, no. 3, pp. 879-921, 1998.
- [16] Fefferman, R. & Kenig, C. & Pipher, J., *The Theory of Weights and the Dirichlet Problem for Elliptical Equations*, Annals of Math. no. 134, pp. 65-124, 1991.
- [17] Golub, G. H. & van Loan, C. E. *Matrix Computations*, The Johns Hopkins University Press; 3rd edition, 1996.
- [18] Grebenkov, D. S. & Beliaev, D. & Jones, P. W., *A Multiscale Guide to Brownian Motion*, Journal of Physics A: Mathematical and Theoretical to appear.
- [19] Holden, P., *Extension Theorems for Functions of Vanishing Mean Oscillation*, Pacific J. Math, 142 (1990), pp. 277-254.
- [20] Jones, P. W., *Factorization of  $A_p$  weights*, Annals of Math. 111 (1980), pp. 511-530.

- [21] Jones, P. W., *Quasiconformal mappings and extendability of functions in Sobolev spaces*, Acta Math. 147(1981), pp. 71-88.
- [22] Jones, P.W., *On Removable Sets for Sobolev Spaces*, in Essays on Fourier Analysis in honor of E.M. Stein, Ed. C. Fefferman, et al. Princeton University Press, 1995, pp. 250-267.
- [23] Jones, P. W. & Maggioni, M. & Schul, R., *Manifold parametrizations by eigenfunctions of the Laplacian and heat kernels*, PNAS vol. 105, no. 6, pp. 1803-1808, 2008.
- [24] Jones, P. W. & Osipov, A. & Rokhlin V., *Randomized Approximate Nearest Neighbors Algorithm*, PNAS vol. 108 no. 38 pp.1567915686, September 20, 2011.
- [25] Kahane, J.-P., *Sur le chaos multiplicative*, Ann. Sci. Math., Quebec, v. 9(2), pp. 105-150, 1985.
- [26] Kolaczyk, E., & Nowak, R., *Multiscale Likelihood analysis and Complexity Penalized Estimation*, The Annals of Statistics, vol. 32, no. 2 (Apr., 2004), pp. 500-527.
- [27] Koller, D., & Friedman, N., *Probabilistic Graphical Models: Principles and Techniques*, The MIT Press, 2009.
- [28] Lerman, G., *Quantifying curvelike structures of measures by using Jones quantities*, CPAM, vol. 56, (8), pp. 1294-1365, 2003.
- [29] Liberty, E. & Martinson, P. & Rokhlin, V. & Tygert, M., *Randomized algorithms for the low-rank approximation of matrices*, PNAS, vol. 104 no. 51, pp. 20167, 2007.
- [30] Maggioni, M. *Geometry of Data and Biology*, Notices of the American Math Society, 62, no. 10 (2015), 1185-1188.
- [31] Mumford, D. & Sharon, E., *2D-Shape Analysis using Conformal Mapping*, Int. J. of Computer Vision, 70, 2006, pp.55-75.
- [32] Ness, L. *Dyadic Product Formula Representations of Confidence Measures and Decision Rules for Dyadic Data Set Samples*, MISNC, SI, DS '16, August 15 - 17, 2016, Union, NJ, USA, isbn 978-1-4503-4129-5/16/08 , <http://dx.doi.org/10.1145/2955129.2955166>.
- [33] Oikawa, K., *Welding of polygons and the type of Riemann surfaces*, Kodai Math. Sem. Rep. vol. 13, no. 1 (1961), pp. 37-52.
- [34] Okikiolu, K., *Characterization of subsets of rectifiable curves in  $R^n$* , J. London Math. Soc. (2) 46 (1992), no. 2, pp. 336-348.
- [35] Osgood, W. F., *A Jordan Curve of Positive Area*, Transactions of the American Mathematical Society, vol. 4, no. 1 (Jan., 1903), pp. 107.-112.
- [36] Rhodes, R. & Vargas, V., *Gaussian multiplicative chaos and applications: a review*, Prob. Surveys, Volume 11 (2014), 315-392.
- [37] Stewart, G. W., *Matrix Algorithms: Volume 1, Basic Decompositions*, SIAM, 1998.
- [38] Stewart, G. W., *Matrix Algorithms: Volume 2, Eigensystems*, SIAM, 2001.

- END -